Inorg. Chem. **2008**, *47*, 8258−8266

Disordered Structures of the TM−Mg−Zn 1/1 Quasicrystal Approximants (TM = Hf, Zr, or Ti) and Chemical Intergrowth

Cesar Pay Gómez,*,† Satoshi Ohhashi,‡ Akiji Yamamoto,§ and An Pang Tsai‡,||

International Center for Young Scientists, International Center for Materials NanoArchitectonics (ICYS-MANA), National Institute for Materials Science (NIMS) 1-1 Namiki, Tsukuba, Ibaraki, 305-0044, Japan, Institute of Multidisciplinary Research for Advanced Materials (IMRAM), 2-1-1 Katahira, Tohoku University, Aoba-ku, Sendai 980-8577, Japan, National Institute for Materials Science (NIMS) 1-1 Namiki, Tsukuba, Ibaraki, 305-0044, Japan, and National Institute for Materials Science (NIMS) 1-2-1 Sengen, Tsukuba, Ibaraki, 305-0047, Japan

Received May 14, 2008

The structures of three quasicrystal approximant phases in the TM−Mg−Zn (TM = Hf, Zr, Ti) systems with the analyzed compositions $Hf_5Mg_{18}Zn_{77}$, $Zr_5Mg_{18}Zn_{77}$, and $Ti_{5.5}Mg_{17.5}Zn_{77}$ have been synthesized, and their structures have been analyzed by single-crystal X-ray diffraction. The structure analyses revealed that these cubic phases with the space group $Pm\bar{3}$ contain two different rhombic-triacontahedral clusters. These clusters are so-called Bergman-type atomic clusters and previously known approximants of face-centered icosahedral (*F*-type) quasicrystals are composed only of Mackay-type clusters, thus these compounds are seen as new prototype structures. Electron density maps calculated by the maximum entropy method (MEM) show that one of the atomic clusters displays characteristic structural disorder. The disorder in these phases is related to the chemical intergrowth of different Friauf polyhedra, and the prospects of new guide lines for finding quasicrystals composed of such polyhedra are discussed.

Introduction

Quasicrystals do not easily lend themselves to structure analysis by conventional methods of X-ray diffraction because their atomic structures lack three-dimensional periodicity. Furthermore, for icosahedral quasicrystals (iQCs), we cannot obtain all the necessary structural information by high-resolution electron microscopy alone, although it can be quite efficient for dihedral quasicrystals (dQCs) which have one periodic direction.[1] Structure refinement is generally performed within the formalism of high-dimensional crystallography (six dimensions for icosahedral quasicrystals), but even so, structures of quasicrystals are difficult to analyze without knowledge of their crystalline approximants. Approximants are periodic crystals which have similar local atomic arrangements (atomic clusters) as those found in the related quasicrystals. Their lattice constants, space groups, and designations (1/1, 2/1, etc.) are also mathematically related to the high-dimensional structure of the parent quasicrystal.[2] To understand the structures of iQCs, it is therefore necessary to first study the detailed structures of approximant phases.[3] This gives important information on local atomic order and cluster arrangements appearing in quasicrystals. If they are classified according to their atomic clusters, there are so far three major families of icosahedral quasicrystals and approximants: Bergman-, Mackay-, and Yb−Cd-type (Tsai-type) phases.[4−7] There are three types of (6-dimensional) icosahedral lattices, these are: primitive

* To whom correspondence should be addressed. E-mail: GOMEZ.Cesar@nims.go.jp.
† International Center for Young Scientists, International Center for Materials NanoArchitectonics (ICYS-MANA), National Institute for Materials Science (NIMS) 1-1 Namiki.
‡ Institute of Multidisciplinary Research for Advanced Materials (IMRAM), Tohoku University.
§ National Institute for Materials Science (NIMS) 1-1 Namiki.
|| National Institute for Materials Science (NIMS) 1-2-1 Sengen.

(1) Hiraga, K. *Adv. Imaging Electron Phys.* **2002**, *122*, 2–68.
(2) Janot, C., In *Quasicrystals: A Primer*, 2nd ed.; Oxford University Press Inc.: Grenoble, France, 1994; pp 1−409.
(3) Henley, C. L.; Elser, V. *Phil. Mag.* **1986**, *B53*, L59–L66.
(4) Bergman, G.; Waugh, J. L. T.; Pauling, L. *Acta Crystallogr.* **1957**, *10*, 254–259.
(5) Kirihara, K.; Nagata, T.; Kimura, K.; Kato, K.; Takata, M.; Nishibori, E.; Sakata, M. *Phys. Rev.* **2003**, *B68*, 014205.
(6) Takakura, H.; Gómez, C. P.; Yamamoto, A.; Boissieu, M. d.; Tsai, A. P. *Nat. Mater.* **2007**, *6*, 58–63.

10.1021/ic800874u CCC: $40.75
Published on Web 08/15/2008

(P-type hereafter), face-centered (F-type), and body-centered (*I*-type) lattices. Among them, F-type Al−Pd−Mn and P-type Cd−Yb quasicrystals have been analyzed in detail.[6,8] Although many other F-type and P-type quasicrystals have been found, their detailed structures are still unknown.

Unfortunately, the existence of quasicrystals does not always guarantee the existence of closely related approximant crystals within the same system, making the task of structural understanding even more difficult. The recent discovery of a new family of Bergman-related phases in the ternary TM−Mg−Zn systems with TM = Hf, Zr or Ti, offers new possibilities to understand the structures and properties of quasicrystals and approximants because of the existence of high quality single crystals.[9] In the investigated TM−Mg−Zn systems, both P- and F-type iQCs and their corresponding 1/1 approximants have been reported. The space group $Pm\bar{3}$ and the lattice constants ∼13.6 Å of the title compounds suggest that they are related with F-type quasicrystals. Thus the phases investigated as part of this work are identified as the 1/1 approximants to the F-type iQCs in the same systems. All reported 1/1 approximants of F-type iQCs to date are composed of Mackay type clusters, with the possible exception of the 1/1 Al−Pd−Mn-Si approximant.[10] The title compounds are thus the first prototype 1/1 approximants of F-type i-QCs to display two distinct and chemically different Bergman type clusters and other unique features which are of considerable importance for understanding the structures of several related quasicrystals.

The structures of 1/1 approximants are generally considered in terms of two building units: the rhombic dodecahedron and the acute rhombohedron.[3] The title compounds can be described in the same way. They can however, also be described in terms of Friauf polyhedra, though in contrast to other Bergman type 1/1 approximants the TM−Mg−Zn phases contain chemically different Friauf polyhedra. Furthermore, these kinds of Friauf polyhedra are found also in Laves phases forming in related binary subsystems with the same chemical decorations. This is the basis for the description of these phases as chemical intergrowth compounds of related Laves phases. Once a stable phase composed of Friauf polyhedra forms in a given system, it is not unusual to find other phases in the same or related systems where this polyhedron reappears but in different arrangements and coexisting with other polyhedra. This point of view leads to a natural interpretation of the disordering appearing in the title compounds and gives rise to the guide line for the formation of quasicrystals, approximants, and other phases. In this paper, the detailed structures of the title compounds with prominent disorder will be clarified and a natural interpretation of the disorder in terms of the chemical intergrowth of Friauf polyhedra will be given. On the basis of considerations of the detailed structures of the title compounds, the prospects of a new guide line for finding other quasicrystal phases will be discussed.

Experimental Section

Syntheses. The approximants and quasicrystals were synthesized by high temperature reaction of the pure constituent elements. The purities of the materials used were Zn (4N), Mg (4N), Ti (3N), Zr (99.5%), and Hf (99.5%). Zn and Mg (shot, 3−5 mm) were used without modification. Ti and Zr (wire, diameter 1.0 mm) were cut to ∼5 mm length. Hf (foil, 0.02 mm) was cut to rectangles ∼1 × 5 mm. The nominal compositions of the product materials (see "Characterization") were inserted into Al_2O_3 crucibles and sealed in silica jackets under Ar atmosphere (∼600 torr). The approximants and P-type quasicrystals were synthesized using an electric muffle furnace at 700 °C for 12 (24) hours, cooled to 500 °C at −3.3 K/min and annealed at 500 °C for 2−5 days. *F*-type single quasicrystals of Zr−Mg−Zn and Hf−Mg−Zn were synthesized as described above, grown by slow-cooling from 700 to 550 °C with a rate of −1 K/h, and subsequently annealed at 550 °C for 7days. Though Ti, Zr, and Hf melt at high temperatures, the samples were never heated above 700 °C to prevent evaporation of Zn. In practice, a Zn−Mg melt will form that acts as a flux for the third element. Because of these synthesis conditions, completely single-phased samples were rarely obtained and impurities of mainly $MgZn_2$ Laves phase were frequently observed in both approximant and quasicrystal samples. The slight compositional differences between the F-type QCs and the approximant phases are very important to take into account to get high yields of the target materials. Long annealing times are also necessary to get single crystals of good quality and sufficient size for X-ray structure analysis.

Characterization. All reaction products were initially identified by powder X-ray diffraction (M03XHF, Mac Science) and selected area electron diffraction (JEM-2000EX, JEOL). The compositions were analyzed using an electron probe microanalyzer (JXA-8621MX, JEOL), which gave the following results: $Hf_5Mg_{18}Zn_{77}$, $Zr_5Mg_{18}Zn_{77}$, and $Ti_{5.5}Mg_{17.5}Zn_{77}$ for the approximants, $Hf_6Mg_{17}Zn_{77}$ and $Zr_{6-6.5}Mg_{18-19}Zn_{75}$ for the F-type QCs, and $Hf_7Mg_9Zn_{84}$ and $Zr_7Mg_{9.5}Zn_{83.5}$ for the P-type QCs. Both powder X-ray diffraction and EPMA measurements confirmed the presence of impurities of $MgZn_2$ and $TMZn_2$ Laves phases, $TMZn_3$ phases, and quasicrystals in some of the samples containing the TM−Mg-Zn 1/1 approximants.

Single crystal data were collected on two different diffractometers; the room temperature measurements on the Ti−Mg−Zn and Zr−Mg−Zn samples were performed using a Rigaku R-axis Rapid II single crystal diffractometer operated at 50 kV, 40 mA with Mo Kα radiation and graphite monochromator. Indexing and empirical absorption correction was performed using the included Rigaku software package. The measurements on the Hf−Mg−Zn sample were performed using a Bruker SMART APEX diffractometer with CCD area detector operated at 40 kV, 40 mA with Mo Kα radiation and graphite monochromator. Indexing and empirical absorption correction was performed using the included Bruker software package (SMART for WNT/2000 5.625 Bruker AXS and SAINT 6.45 SADABS). Low-temperature single-crystal measurements at 120 K for the Hf−Mg−Zn sample were performed on the same Bruker diffractometer using a Japan Thermal Engineering Co., Ltd., XR-HR10K cryostat with liquid nitrogen flow.

(7) Tsai, A. P.; Guo, J. Q.; Abe, E.; Takakura, H.; Sato, T. J. *Nature* **2000**, *408*, 537–538.
(8) Yamamoto, A.; Takakura, H.; Tsai, A. P. *Phys. Rev.* **2003**, *B68*, 094201.
(9) Hasegawa, J.; Takeuchi, S.; Tsai, A. P. *Phil. Mag. Lett.* **2005**, *85*, 289–297.
(10) Sugiyama, K.; Kaji, N.; Hiraga, K. *Z. Kristallogr.* **1998**, *213*, 168–173.

Table 1. Crystallographic Information for the Refined TM−Mg−Zn Approximants (TM = Hf, Zr, Ti)

refined composition	$Hf_{1.136}$ $Mg_{4.215}$ $Zn_{21.076}$	$Zr_{1.149}$ $Mg_{3.946}$ $Zn_{21.336}$	$Ti_{1.361}$ $Mg_{3.994}$ $Zn_{20.968}$
normalized composition (%)	$Hf_{4.30(2)}$ $Mg_{15.9(2)}Zn_{79.8(4)}$	$Zr_{4.35(5)}$ $Mg_{14.9(2)}$ $Zn_{80.7(7)}$	$Ti_{5.17(5)}$ $Mg_{15.2(2)}Zn_{79.7(7)}$
molar mass (g)	1683.2	1595.7	1533.1
temp (K)	295	295	295
space group	$Pm\bar{3}$	$Pm\bar{3}$	$Pm\bar{3}$
lattice constant a (Å)	13.6740(11)	13.7090(5)	13.5541(8)
cell vol (Å^3)	2556.7(4)	2576.42(16)	2490.1(3)
Z	6	6	6
calcd density (g cm^{-3})	6.5569	6.1686	6.1323
abs coeff μ (mm^{-1})	36.013	29.929	30.376
independent reflns	1441	1113	1083
independent reflns obsd [$I > 3\sigma(I)$]	903	617	864
R_{int} (obs/all)	0.0759/0.0857	0.1398/0.1853	0.1102/0.1151
params	128	118	119
R1/wR2 (obsd)[a]	0.0373/0.0688	0.0580/0.1003	0.0357/0.0799
R1/wR2 (all)[a]	0.0735/0.0726	0.1043/0.1108	0.0469/0.0836
GOF on F^2 (obsd/all)	1.90/1.55	2.05/1.60	1.69/1.55
$\Delta\rho_{min}$, $\Delta\rho_{max}$ [e Å^{-3}]	2.66, −2.22	5.08[b], −2.69	1.45, −1.30

[a] $R1 = \Sigma||F_o| - |F_c||/\Sigma|F_o|$; $wR2 = \{[\Sigma[w(F_o^2 - F_c^2)^2]/\Sigma[w(F_o^2)^2]]\}^{1/2}$. [b] The highest residual peak is located at the high-symmetry position 1/2, 1/2, 1/2, at 1.96−2.26 Å distance from the disordered positions Zn17−19.

The program JANA2006 was used for the structure refinements.[11] Electron density maps were calculated by the maximum entropy method (MEM) software included as part of the REMOS program package.[12−14] The structures and electron density iso-surfaces were visualized using the programs VESTA 1.3.1,[15] Diamond 3.1f,[16] and Caligari Truespace 7.51.[17]

Refinement. Electron diffraction and powder diffraction experiments revealed that the diffraction patterns of the title compounds could be indexed with primitive cubic unit cells; the relation between their lattice constants and the icosahedral lattice constants of the parent F-type (face-centered icosahedral) quasicrystals obey the formula $a_{AP} = a_{QC}(4 + 8/\sqrt{5})^{1/2}$, where a_{AP} is the lattice constant of the cubic approximant and a_{QC} is the "quasilattice constant" of the corresponding quasicrystal as defined by V. Elser.[18] For a 1/1 approximant of an F-type quasicrystal, we would usually expect the space group $Pm\bar{3}$. However, by direct methods an appropriate initial structure solution could only be obtained in the non-centrosymmetric space group $P23$. The structure was first solved in $P23$, and after careful analysis it was deemed that there was nothing in the structure breaking the centrosymmetry. Thus, the symmetry was again increased to $Pm\bar{3}$ and the subsequent refinement proceeded smoothly. In the initial refinement of the Hf-containing phase, the goodness of fit parameter and overall R-factors were high (GOF ≈ 3.6, wR2 ≈ 16%); the problem could be solved by omitting the two nonmatching reflections 001 and 011 from the refinement. In doing so, the values dropped down to the final values GOF = 1.55 and wR2 = 7.26%. (The problem was only observed in the data collected on the Bruker CCD diffractometer, which gave unrealistically low intensities and σ-values for these two low-angle reflections.) Extinction parameters were refined. However, the effect of extinction was deemed negligible likely because of the inherent imperfections and disorder of the structures (in fact the refined extinction parameter was somewhat negative because the calculated intensities of some of the strongest peaks were between 2−5% weaker than the observed intensities, this could be caused by poor absorption correction because the empirical method can be ineffective for crystals with highly irregular shape). All atoms were refined with anisotropic displacement parameters except for the split positions Zn17 and Zn19 that were refined isotropically and the disordered positions Zn7, Zn8/Mg8, and Zn15 that were refined with fourth- and third-order anharmonic tensors. The addition of anharmonic tensors helps to model more complex electron density distributions because it is a further parametrization of the thermal displacement. A second-order anharmonic tensor corresponds to an individual anisotropic temperature parameter.

Weak superlattice reflections were sometimes observed by electron diffraction in samples of the Ti−Mg−Zn approximant phase with slightly different composition, no superstructure could however be detected using a conventional laboratory X-ray source. This suggests that superlattice ordering could exist within smaller domains (short or medium range order). Crystallographic data for all three TM−Mg−Zn phases is listed in Table 1 and in the Supporting Information, and refined structural parameters are listed in Table 2.

Results

Disordered Structures and their Descriptions. The three TM−Mg−Zn phases have many structural features in common. However, some differences can be seen and though most of the atomic positions are well-defined, some positions exhibit both positional and chemical disorder thus introducing certain arbitrariness in the structural interpretation. The analyzed compositions ($Hf_5Mg_{18}Zn_{77}$, $Zr_5Mg_{18}Zn_{77}$, and $Ti_{5.5}Mg_{17.5}Zn_{77}$) indicate a slightly lower Zn content than seen in the refinement results ($Hf_{4.30(2)}Mg_{15.9(2)}Zn_{79.8(4)}$, $Zr_{4.35(5)}$-$Mg_{14.9(2)}Zn_{80.7(7)}$, and $Ti_{5.17(5)}Mg_{15.2(2)}Zn_{79.7(7)}$). Further chemical mixing is entirely possible; however, the inherent disorder of these phases prevents a more detailed refinement. Chemical and positional disorder is very often observed in quasicrystals and approximants. This fact that raises the question of whether such structural and chemical flexibility is a necessary component in their formation.[19]

In the context of quasicrystals it is preferable to describe the title compounds in terms of atomic shells and clusters for the purpose of structure analysis. However, in this case

(11) Petricek, V.; Dusek, M.; Palatinus, L. *Jana2006*: Structure Determination Software Programs: Praha, Czech Republic, 2006.
(12) Yamamoto, A. *Acta Crystallogr.* **1982**, *A38*, 87–92.
(13) Yamamoto, A. *Ferroelectrics* **2001**, *250*, 139–142.
(14) Sakata, M.; Sato, M. *Acta Crystallogr.* **1990**, *A46*, 263–270.
(15) Momma, K.; Izumi, F. *IUCr Newslett.* **2006**, *7*, 106–119.
(16) Brandenburg, K.; Putz, H. *Diamond*, 3.1f; Crystal Impact: Bonn, Germany, 2008.
(17) Ormandy, R. *Truespace*, 7.51; Caligari Corporation: Mountain View, CA, 2007.
(18) Elser, V. *Phys. Rev.* **1985**, *B32*, 4892–4898.
(19) Henley, C. L., In *Quasicrystals: The State of the Art*; DiVincenzo, D. P.; Steinhardt, P., Eds. World Scientific: Singapore, 1991; p 429.

Table 2. Refined Atomic Positions, Occupancies and Equivalent Isotropic Displacement Parameters for the TM−Mg−Zn Approximants (TM = Hf, Zr, Ti)

TM metal	atom	Wyckoff	SOF	*x*	*y*	*z*	U_{eq} (Å^2)[a]
Hf	Hf1	6g	1	0.30315(4)	0.5	0	0.00944(18)
Zr	Zr1	6g	1	0.30402(16)	0.5	0	0.0150(7)
Ti	Ti1	6g	1	0.30124(15)	0.5	0	0.0093(6)
Hf	Mg2	12j	1	0.3086(2)	0.1170(2)	0	0.0129(10)
Zr	Mg2	12j	1	0.3094(4)	0.1166(4)	0	0.0218(19)
Ti	Mg2	12j	1	0.3094(2)	0.1178(2)	0	0.0119(9)
Hf	Mg4/Hf4	8i	0.898/0.102(3)	0.18855(10)	0.18855(10)	0.18855(10)	0.0129(5)
Zr	Mg4/Zr4	8i	0.888/0.112(9)	0.1887(2)	0.1887(2)	0.1887(2)	0.0219(12)
Ti	Mg4/Ti4	8i	0.729/0.271(12)	0.18987(12)	0.18987(12)	0.18987(12)	0.0137(5)
Hf	Zn1	12j	1	0.09602(8)	0.15563(8)	0	0.0110(3)
Zr	Zn1	12j	1	0.09620(14)	0.15614(13)	0	0.0196(6)
Ti	Zn1	12j	1	0.09732(7)	0.15583(7)	0	0.0113(3)
Hf	Zn3	24l	1	0.19090(6)	0.40626(6)	0.16214(6)	0.0158(3)
Zr	Zn3	24l	1	0.19079(11)	0.40627(10)	0.16219(10)	0.0244(5)
Ti	Zn3	24l	1	0.19222(5)	0.40655(5)	0.16262(5)	0.0170(3)
Hf	Zn5	6g	1	0.09277(12)	0.5	0	0.0172(5)
Zr	Zn5	6g	1	0.0924(2)	0.5	0	0.0270(10)
Ti	Zn5	6g	1	0.09417(10)	0.5	0	0.0164(5)
Hf	Zn6	24l	1	0.35283(6)	0.31587(6)	0.09906(6)	0.0188(3)
Zr	Zn6	24l	1	0.35291(11)	0.31510(11)	0.09911(10)	0.0276(5)
Ti	Zn6	24l	1	0.35392(6)	0.31803(5)	0.09887(5)	0.0193(3)
Hf	Zn7	12k	1	0.2314(4)	0.5	0.3433(3)	0.0650(17)
Zr	Zn7	12k	1	0.2368(6)	0.5	0.3483(4)	0.088(3)
Ti	Zn7	12k	1	0.2335(2)	0.5	0.3425(2)	0.0491(13)
Hf	Zn8/Mg8	12k	0.967/0.033(9)	0.3686(3)	0.5	0.2008(2)	0.0443(7)
Zr	Zn8/Mg8	12k	0.980/0.020(11)	0.3665(3)	0.5	0.2045(3)	0.0487(11)
Ti	Zn8/Mg8	12k	0.999/0.001(7)	0.3764(2)	0.5	0.1926(2)	0.0468(6)
Hf	Zn10/Mg10	6f	0.833/0.167(11)	0	0.5	0.20424(15)	0.0243(8)
Zr	Zn10/Mg10	6f	0.885/0.115(12)	0	0.5	0.2044(2)	0.0314(13)
Ti	Zn10	6f	1	0	0.5	0.20504(12)	0.0219(5)
Hf	Zn13	12j	1	0.18553(8)	0.31576(8)	0	0.0138(4)
Zr	Zn13	12j	1	0.18559(14)	0.31555(14)	0	0.0229(7)
Ti	Zn13	12j	1	0.18648(7)	0.31605(7)	0	0.0136(3)
Hf	Zn14	6h	0.5	0.5	0.5	0.1086(4)	0.088(3)
Zr	Zn14	6h	0.5	0.5	0.5	0.1086(5)	0.092(5)
Ti	Mg14/Zn14	6h	0.396/0.104(10)	0.5	0.5	0.1069(5)	0.041(3)
Hf	Zn15	12k	0.5	0.5	0.4089(4)	0.031(4)	0.079(13)
Zr	Zn15	12k	0.5	0.5	0.4080(3)	0.0421(4)	0.061(3)
Ti	Zn15	6f	1	0.5	0.4090(3)	0	0.0976(14)
Hf	Mg12/Zn12	8i	0.588/0.412(11)	0.3118(3)	0.3118(3)	0.3118(3)	0.0387(7)
Zr	Mg12/Zn12	8i	0.455/0.545(12)	0.31031(19)	0.31031(19)	0.31031(19)	0.0423(10)
Ti	Mg12/Zn12	8i	0.467/0.533(8)	0.31333(11)	0.31333(11)	0.31333(11)	0.0382(5)
Hf	Zn17	24l	0.077(3)	0.4050(16)	0.3867(11)	0.4248(10)	0.028(5)
Zr	Zn17	24l	0.091(9)	0.407(4)	0.386(2)	0.426(2)	0.049(10)
Ti	Zn17	24l	0.078(3)	0.402(2)	0.3903(16)	0.4282(12)	0.053(7)
Hf	Zn18	12k	0.368(14)	0.3514(6)	0.5	0.5439(9)	0.120(6)
Zr	Zn18	12k	0.42(3)	0.3623(12)	0.5	0.5495(14)	0.173(16)
Ti	Zn18	12k	0.34(2)	0.3505(6)	0.5	0.5298(10)	0.122(10)
Hf	Zn19	12k	0.108(12)	0.5	0.3671(17)	0.436(2)	0.063(11)
Zr	Zn19	12k	0.028(17)	0.5	0.372(7)	0.436(6)	0.01(4)
Ti	Zn19	12k	0.08(2)	0.5	0.364(3)	0.435(3)	0.058(16)

[a] $U_{eq} = (U_{11} + U_{22} + U_{33})/3$.

such a description fails to capture the underlying chemical simplicity of these compounds, and we will thus also include a second description which emphasizes the structural and chemical relation to different Frank−Kasper phases.[20,21]

Atomic Shell Description. Because of the structural similarities between the three TM−Mg−Zn (TM = Hf, Zr, or Ti) phases, we will use the Hf−Mg−Zn structure as a prototype for the structural descriptions and mention the Zr- and Ti-containing phases only when significant differences are present in these structures.

The structures of the three title compounds can be described in terms of packings of rhombic triacontahedral clusters (RTHs). Two types of RTH clusters exist in these compounds; one at the body center (B-RTH) and the other at the vertex (V-RTH) of the cubic unit cell. Although both cluster types can be categorized as Bergman clusters,[4] they are different both with respect to chemical and positional order/disorder. The atomic shells of the two clusters are displayed in Figure 1 a−d.

Starting from the innermost atomic shells and going outward, we can describe the shells as follows: The first shell of the V-RTH is an almost perfect icosahedron composed entirely of Zn atoms (position Zn1), and in the B-RTH, the first shell is also composed of Zn (positions Zn17, Zn18, Zn19) but exhibits severe positional disorder (Figure 1a).

(20) Frank, F. C.; Kasper, J. S. *Acta Crystallogr.* **1958**, *11*, 184–190.
(21) Frank, F. C.; Kasper, J. S. *Acta Crystallogr.* **1958**, *12*, 483–499.

The second shells are seen in Figure 1b. In the V-RTH, we find two shells: a dodecahedron composed almost exclusively of Mg with a minor amount of TM (positions Mg2, and Mg4/TM4) and an icosahedron composed entirely of Zn (Zn13). The dodecahedron composed of Mg and a minor amount of TMs is the most prominent difference in chemical composition between the two V-RTH and B-RTH clusters. In the V-RTH, this dodecahedron defines the 3-fold vertices of a rhombic triacontahedron and the Zn13 icosahedron defines the 5-fold vertices.

In the B-RTH, we also find a dodecahedron (Zn8/Mg8 and Zn12/Mg12) and an icosahedron (Zn7). In this case however, they are both mostly composed of Zn, although some chemical mixing with Mg occurs at the dodecahedral sites, particularly, those located on 3-fold symmetry axes (Zn12/Mg12). The Zn icosahedron has no chemical mixing, but it exhibits positional disorder. The average size of the Zn7 icosahedron in the B-RTH is smaller than that of the Zn13 icosahedron in the V-RTH; however, because of the positional disorder the size of the Zn7 icosahedron cannot be determined accurately.

The third shells in both V-RTH and B-RTH clusters form soccer ball-polyhedra composed of Zn (Figure 1c). In the V-RTH, the soccer ball is defined by the atomic positions Zn3, Zn5, and Zn6 and, in the B-RTH, by Zn3, Zn6 and Zn15. The atomic position Zn15 together with Zn14 defines a positional disorder that gives rise to an unusual doughnut-shaped electron density found centering every face of the unit cell. In the Ti-containing phase, this disorder has a somewhat different shape and there is substantial mixing of Mg into the Zn14 position. The description of this disorder is described in detail under "chemical and positional disorder".

The sequence of atomic shells described so far is typical for the well-known Bergman type cluster. Both the V-RTH and B-RTH clusters can be classified as being of Bergman type, although the B-RTH displays severe disorder. However, it is obvious in these structures that the atomic shells generally included in the Bergman description are not sufficient to fully describe the clusters of the title compounds since this description fails to include the TMs (Hf, Zr, and Ti) as part of the cluster. Thus these atoms would be seen as "glue atoms" and be a source of complication when trying to model the structures of corresponding quasicrystals.[22] This problem has recently been overcome in the structure refinement of the binary icosahedral phase $YbCd_{5.7}$ by expansion of the boundary of the cluster to include glue atom regions and allowing the clusters to interpenetrate.[6] The method is also applicable to other Bergman type approximants, and in all cases the clusters can be described as rhombic triacontahedra with different atomic decorations.[23,24] Following the same procedure for the TM−Mg−Zn phases, we can include the TM elements as part of the cluster by using the rhombic triacontahedral description. Thus the outermost shells of the clusters are RTH units with mainly Zn and TMs at the vertices. In the V-RTH, the TM (Hf1) atoms are located at the 5-fold vertices of the triacontahedron, while mostly Zn (Zn10/Mg10, Zn12/Mg12) atoms occupy the 3-fold vertices. In the B-RTH, the situation is reversed; TM atoms (Hf1, Mg4/Hf4) occupy 3-fold vertices and Zn atoms (Zn10/Mg10) occupy the 5-fold (Figure 1d).

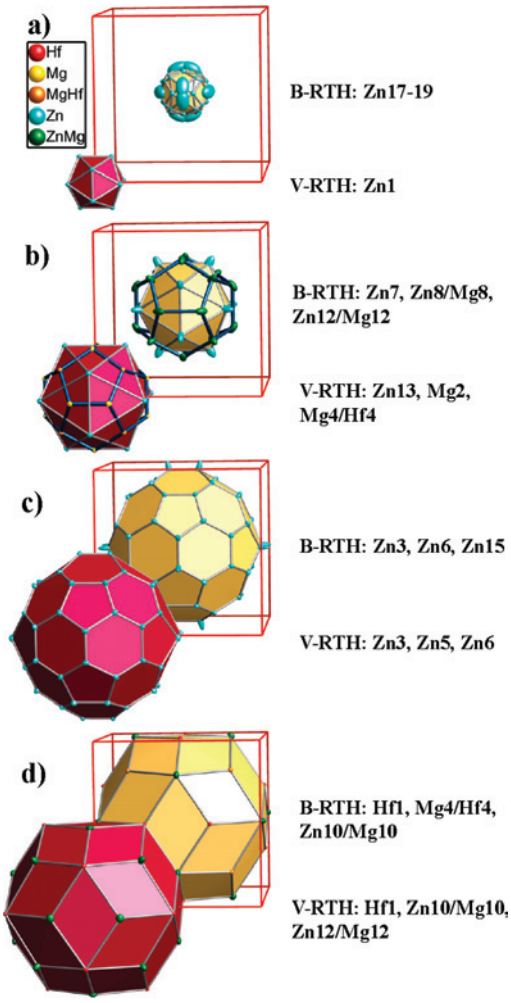

Figure 1. (a−d) Successive atomic shells of the two symmetry independent cluster units at the vertex (V-RTH) and body center (B-RTH) of the cubic unit cell. All atomic positions are displayed with thermal ellipsoids at the 70% probability level. Atom type color codes are indicated by the legend and the atomic positions comprising each shell are listed.

Chemical and Positional Disorder. The way to model some of the complex disorder in the refinements of the three TM−Mg−Zn phases can vary depending on several factors; in some cases, for example, a split position approach may result in a more stable refinement, compared to a single atomic position description, with large thermal displacement parameters or vice versa. The positional disorder of the title compounds is seen in Figure 2a−g, where electron density maps of the structures calculated by the maximum entropy method are shown (thermal ellipsoids colored in light blue are superimposed).

The positional disorder in the TM−Mg−Zn phases is mostly confined to the B-RTH cluster, while the V-RTH is

(22) Thiel, P. *Nat. Mater.* **2007**, *6*, 11–12.
(23) Lin, Q.; Corbett, J. D. *Proc. Nat. Acad. Sci.* **2006**, *103* (37), 13589–13594.
(24) Audier, M.; Pannetier, J.; Leblanc, M.; Janot, C.; Lang, J. M.; Dubost, B. *Physica* **1988**, *B153*, 136–142.

a typical Bergman cluster devoid of positional disorder. The central core units of the B-RTH clusters exhibit the most severe forms of positional disorder (Figure 2d−f); the highest electron densities for these units are found near the vertices defined by two superimposed pentagonal dodecahedra rotated by 90° along a common 2-fold axis with respect to each other (Figure 2 d). As a consequence of unreasonably short interatomic distances, these two dodecahedral orientations are mutually exclusive; furthermore only about 7 Zn atoms are distributed over the total of 32 vertices (in fact the vertices colored in red are only located near 3-fold symmetry axes and are thus split into three equivalent positions).

Another disordered shell of the B-RTH is the mentioned icosahedron defined by the Zn7 position (blue electron densities in Figure 2a−c). The elongated densities indicate a "breathing" motion of the icosahedron where the vertices move toward or away from the center of the cluster. This "breathing" can be correlated to the positional disorder of the central core unit, which strongly seems to affect the Zn7 position. Other atomic positions at similar distances from the cluster center such as the dodecahedron defined by Zn8/Mg8 and Zn12/Mg12 are also affected and can in addition exhibit chemical mixing (yellow and green electron densities respectively in Figure 2 a-c).

Despite the similarity in atomic size between Hf, Zr, and Mg, the structures show a quite well-defined chemical order between the TM metals and Mg. Only the Mg4/TM4 positions are mixed between the two. The Mg4/TM4 and Mg12/Zn12 positions are the only ones located on the 3-fold symmetry axes; these positions often display deviating behavior in terms of occupancy also in several other approximant phases.[10,25] In the case of the TM−Mg−Zn phases the chemical mixing between the TM-metals and Mg can be understood if we consider that the Mg4/TM4 position is the shared linking vertex between two different dodecahedral shells: one composed of Mg and the other of TM. As a result this linking position is mixed between the two species. The Mg12/Zn12 position also forms the link between two different dodecahedra; however these dodecahedra are mostly composed of Zn, with the exception of the mentioned Mg12/Zn12 position, which always has a large content of Mg.

The Hf−Mg−Zn sample was also measured at 120 K. The refinement against the low-temperature data overall showed little change in the structural parameters other than the expected decrease in lattice constants and thermal displacement parameters. For atomic positions with positional disorder, however, the thermal displacement parameters and electron densities showed no significant decrease in magnitude along the main directions of elongation in contrast to all other atomic positions, which show a typical isotropic contraction. This indicates that the positional disorder is essentially unaffected by the temperature change and thus has little to do with thermal motion. In other words, the disorder is likely to be static in nature because we would not expect anything but a decrease in thermal motion with decreasing temperature.

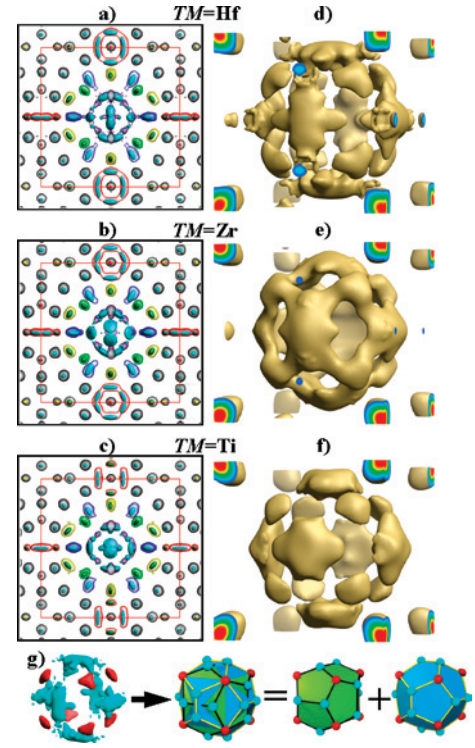

Figure 2. Superimposed thermal ellipsoids and electron density isosurfaces calculated by MEM for the three TM−Mg−Zn phases (TM = Hf in a, Zr in b, and Ti in c). In a−c, the sections are shown within the unit cell limits $-0.15 \le x, y \le 1.15$, $0.25 \le z \le 0.75$. Note that the shown atoms are not all in the same plane. The thermal ellipsoids (nontransparent) are shown at the 70% probability level and the isosurfaces (transparent) at the 6.5 e Å^{-3} isolevel. Isosurfaces corresponding to disordered positions are seen in different colors (green = Zn12/Mg12, yellow = Zn10/Mg10, blue = Zn7, purple = Zn17−19, red = Zn14,15) and ordered positions in dark gray. In d−f, the isosurfaces of the corresponding disordered core units are shown in perspective view, unit cell limits $0.3 \le x, y, z \le 0.7$ and isolevels at 4.0 e Å^{-3}. In g, a schematic interpretation of the core disorder is shown. The highest electron densities are found near the vertices of two superimposed dodecahedra, rotated by 90° with respect to each other.

Although the three title compounds have most structural features in common, it can be seen that the electron density distributions and the chemical mixing behavior at individual atomic sites vary between them. The Ti−Mg−Zn phase in particular differs from the Hf- and Zr-containing phases in several ways: The positions Zn10/Mg10 and Zn8/Mg8 have no significant mixing of Mg. The absence of Mg at these sites in the Ti-containing phase is balanced by mixing of Mg into the Zn14 position, resulting in a rather similar composition for all three phases. Overall, the refined compositions tend to be somewhat Mg deficient and have a slight Zn surplus compared to the experimentally analyzed ones (about 3 atom % difference); this indicates that some additional mixing of Mg into Zn positions might occur, but this is difficult to refine with accuracy because of the strong correlations between temperature and occupancy parameters in these disordered structures. In Figure 2c, it is clearly seen that the doughnut-shaped electron density (red electron densities in Figure 2a−c) defined by Zn14 and Zn15 also

(25) Gómez, C. P.; Lidin, S. *Phys. Rev.* **2003**, *B 68*, 024203(1)-024203(9).

has a different shape in the Ti-containing phase as compared to the Hf- and Zr-containing phases.

It should be mentioned that the exact composition of the species residing at the Zn14 position cannot be ascertained by single crystal diffraction techniques. An equally valid refinement is obtained by introducing a partially occupied Zn atom at this position instead of mixing with Mg. However, opting for a mixed Zn/Mg position agrees better with the experimentally observed composition for the Ti-containing phase. These doughnut-shaped electron densities can be modeled in different ways, but the interpretation remains that they arise as a consequence of rotational disorder of a triangular face belonging to the coordination polyhedron (Friauf polyhedron) around the TM atoms Hf1, Zr1, and Ti1. From a crystal-chemical point of view, most of the structural framework of the title compounds and also the disorder can be understood by regarding the structures as chemical intergrowth compounds of structurally related Frank−Kasper phases as explained in the following section.

Chemical Intergrowth: A Link to Related Frank−Kasper Phases. It was already observed by F. C. Frank and J. S. Kasper that the Bergman type 1/1 approximant in the Al−Mg−Zn system could be described in terms of the basic atomic layers and polyhedra that they had defined for certain tetrahedrally close-packed structures (tcp).[21] S. Andersson introduced the concept of chemical twinning; relating Laves phases to other known structures by certain symmetry operations.[26] Furthermore S. Samson described several tcp structures in terms of one of these polyhedra, which he named the Friauf polyhedron.[27] The Friauf polyhedron is a truncated tetrahedron with hexagonal and triangular faces, decorated with atoms at the vertices, a central atom, and capping atoms on each hexagonal face (seen in different arrangements in Figure 3a−c). These observations were mainly geometrical and mathematical in nature, and we here wish to emphasize their chemical meaning.

The description of the three TM−Mg−Zn phases as chemical intergrowth compounds composed of Friauf polyhedra from the related Laves phases $MgZn_2$, and one of the three Laves phases $HfZn_2$, $ZrZn_2$, and $TiZn_2$ is depicted in Figure 3a.[28−30] Furthermore, most of the chemical and positional disorder in the title compounds can be understood by applying exchange mechanisms (for the chemical disorder) and a rotational mechanism (for the positional disorder) to these Friauf polyhedra (Figure 3b and c). The chemical disorder is simply caused by stacking faults where one type of Friauf polyhedron is locally replaced by another with a different chemical decoration. The chemical disorder between TMs and Mg can easily be understood by exchanging Friauf polyhedra from the $MgZn_2$ phase by those from the corresponding $TMZn_2$ phase. This however, does not account for the chemical mixing between Mg and Zn which has to be explained by a second exchange mechanism described below.

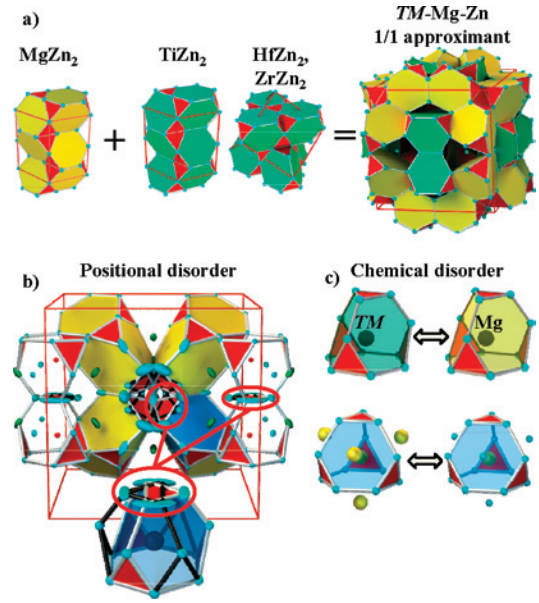

Figure 3. Chemical intergrowth and disorder described with Friauf polyhedra in the TM−Mg−Zn phases (TM = Hf, Zr, Ti). In a, the schematic intergrowth of the structures using building blocks from related Laves phases is shown. In b, a rotational mechanism is used to reproduce the disorder of the central core units and doughnut-shaped electron densities of the title compounds. The lower inset shows the two possible orientations of the Friauf polyhedron, one orientation is outlined by white bonds and the other by black. The two orientations are rotated by 180° with respect to each other around a common 3-fold axis of the polyhedron. The effect of the rotation can only be seen in the areas marked by red ellipses; these indicate the locations of two staggered triangular faces forming a hexagon. In c, the chemical disorder is shown in the upper inset as an exchange of Friauf polyhedra centered by TM-metals and Mg. The lower inset in c (rotated view), shows the chemical decorations of two Friauf polyhedra including capping atoms, as they appear in Laves phases (lower left image) and $AuBe_5$-type phases (lower right image). The chemical Mg/Zn mixing of capping atoms in the TM−Mg−Zn phases can be reproduced by allowing either of these two decorations locally, with Zn atoms = blue and Mg atoms = yellow.

In Laves phases, the hexagonal faces of the Friauf polyhedra are always capped by the same atomic species that resides in the center of the polyhedron. In phases that conform to the structure type described by the prototype $BeAu_5$, however,[31] these capping atoms are of the same type as the vertex atoms of the Friauf polyhedron and are thus different compared to the central atom. By exchanging these two types of Friauf polyhedra, we can reproduce the chemical mixing between Mg and Zn as illustrated in the lower inset of Figure 3c. This mechanism implies that Mg/Zn mixing always occurs at atomic positions capping hexagonal faces of Friauf polyhedra. The situation is particularly intriguing for atoms belonging to the dodecahedral shell (Figure 1b) of the B-RTH cluster (Zn8/Mg8 and Zn12/Mg12) because all these atoms simultaneously play the roles of central atoms and capping atoms of adjacent Friauf polyhedra. It should however be noted that no phase conforming to the $BeAu_5$ structure type has been reported in the binary Mg−Zn system.

Most of the positional disorder of the central core units and the doughnut-shaped electron densities centering the unit cell faces can surprisingly be explained by only one

(26) Andersson, S. *J. Solid State Chem.* **1978**, *23*, 191–204.
(27) Samson, S., The structure of complex intermetallic compounds. In *Structural Chemistry and Molecular Biology*; Rich, A.; Davidson, N., Eds. Freeman: San Francisco, CA, 1968; pp 687−717.
(28) Laves, F.; Witte, H. *Metallwirtsch. Metallwiss. Metalltech.* **1935**, *14*, 645–649.
(29) Robteutscher, W.; Schubert, K. *Z. Metallkd.* **1965**, *56*, 730–734.
(30) Pietrokowsky, P. *Trans. Am. Inst. Min. Metall. Pet. Eng.* **1954**, *200*, 219–226.

mechanism: a 180° rotation of a Friauf polyhedron around its inherent 3-fold axis. These procedures are illustrated in Figure 3b and c. The two orientations of this Friauf polyhedron are mutually exclusive because of short interatomic distances. Thus it is possible to have perfect local positional and chemical order and still obtain the chemical mixing and positional disorder merely as an outcome of the weighted average structure.

Discussion

Laves phases and other related Frank−Kasper phases play an important role in the context of quasicrystals because the Friauf polyhedron is an important building block of the Bergman type and Yb−Cd type phases.[6,32] A Bergman cluster can be entirely described as a union of 20 Friauf polyhedra,[27] and in the Yb−Cd type phases, the acute rhombohedron defined by two face-sharing Friauf polyhedra is regarded as one of the fundamental units that can specify the structures of the 2/1 approximant and the icosahedral phase. The concept of chemical intergrowth does thus not only apply to Bergman-type phases but can also be expanded to Yb−Cd type phases, where we also often see the existence of Laves phases going hand in hand with the formation of the related quasicrystals. The Yb−Cd system is a perfect example. Even though Yb−Cd type 1/1 approximant structures form in all the RE−Cd (RE = rare earth) systems; quasicrystals form only in the RE−Cd system where a Laves phase also forms: the Yb−Cd system (this is also true for the Ca−Cd system). The structures of both the Yb−Cd 2/1 approximant and the *i*-$YbCd_{5.7}$ quasicrystal can be seen as chemical intergrowths of the Laves phase $YbCd_2$ and the 1/1 approximant $YbCd_6$ because they can be described as mixtures of building blocks of these two phases (Yb−Cd type 1/1 approximants in turn can be seen as chemical twins of the related $RE_{13}(Zn/Cd)_{58}$ phases).[33,34] Seeing quasicrystals and approximants as balanced intergrowth compounds composed of building blocks found in other related phases could let us understand the chemical reasons for their formation and observed phenomena such as the relation between quasicrystals and "cluster lines".[35] In the light of this fact, the question arises whether it is possible to regard Laves phases as quasicrystal approximants. Though they may not fulfill the strict mathematical conditions of the definition, the high dimensional relation between Laves phases and Frank-Kasper type quasicrystals was already discussed by Q. B. Yang and K. H. Kuo.[36] Furthermore, from a chemical point of view the Laves phases certainly satisfy the condition of having similar local atomic arrangements as those found in the corresponding quasicrystals; for both Bergman and Yb−Cd-type phases.

In the case of the TM−Mg−Zn (TM = Hf, Zr, or Ti) phases, they can all be seen as chemical intergrowth structures of two different Laves phases in their corresponding binary subsystems: the Mg−Zn system on one hand and the corresponding TM−Zn system on the other. In the Mg−Zn system, we find the Laves phase $MgZn_2$, which is the hexagonal prototype structure for such phases. In the binary Hf−Zn and Zr−Zn systems, the cubic Laves phases $HfZn_2$ and $ZrZn_2$ form ($MgCu_2$ type), while the Ti−Zn system contains the phase $TiZn_2$, which is isostructural to $MgZn_2$. Furthermore, the nature of the chemical and positional disorder is clarified when the structures are described in terms of Friauf polyhedra. Most of this complicated disorder can elegantly be explained by two simple mechanisms; the rotation of certain Friauf polyhedra and the exchange between these polyhedra.

The TM−Mg−Zn quasicrystals and approximants were discovered as a sequence of compounds generated from the Sc−Mg−Zn phases by chemical substitution, and it was expected that the structures in these alloy systems would be identical.[37] However, as described above the structures of the icosahedral clusters in the TM−Mg−Zn phases (TM = Hf, Zr, Ti) are completely different from those of the Sc−Mg−Zn phases, which are of Yb−Cd type. On the other hand, the TM content of the approximants and the quasicrystals in the title systems is almost half-that of Sc, and the TMs are formally regarded as tetravalent as opposed to Sc which is trivalent. The TM content results in rather similar e/a concentrations (∼2.1) for the two systems.

It is well-known that the valence electron concentration (e/a) is one of the most important parameters for the stabilization of quasicrystal structures. It can thus be speculated that to (satisfy Hume−Rothery rules) keep the same e/a concentration, the compositions of the title compounds change and concurrently this induces a change in the structure of the icosahedral cluster. As mentioned previously, many quasicrystals exist, detailed structures of which are unknown. Nevertheless, we still have the possibility to find new quasicrystals with interesting properties. The new guideline proposed in this paper is that if binary Laves phases exist in different alloy systems with one element in common, the ternary system that links the two subsystems together is of potential interest provided that also other factors such as e/a ratio are satisfied. The approach also suggests that if a Laves phase coexists with the structure of a 1/1 approximant in a given system, the existence of a quasicrystal phase is also highly likely.

Summary and Concluding Remarks

Three 1/1 approximants in Hf−Mg−Zn, Zr−Mg−Zn, and Ti−Mg−Zn systems have been synthesized, and their detailed structures have been clarified by single-crystal X-ray analysis. All the approximants have disordered atomic sites in similar positions. To interpret the disordering, the structures are described with two kinds of Friauf polyhedra with

(31) Misch, L. *Metallwirt. Metallwiss. Metalltech.* **1935**, *14*, 897.
(32) Gómez, C. P., Analysis of the $M_{13}Cd_{76}$ phases (M = Ca or Yb). In *Order and Disorder in the RE−Cd and Related Systems*; Stockholm University: Stockholm, Sweden, 2003; pp 54−64.
(33) Gómez, C. P.; Lidin, S. *Solid State Sci.* **2002**, *4*, 901–906.
(34) Palenzona, A. *J. Less-Common Met.* **1971**, *25*, 367–372.
(35) Dong, C.; Wang, Q.; Chen, W.; Zhang, Q.; Qiang, J.; Wang, Y. *J. Univ. Sci. Technol. Beijing* **2007**, *14* (1), 1–3.
(36) Yang, Q. B.; Kuo, K. H. *Acta Crystallogr.* **1987**, *A43*, 787–795.
(37) Ishimasa, T.; Kaneko, Y.; Kaneko, H. *J. Non-Cryst. Solids* **2004**, *334&335*, 1–7.

different atomic decorations. The structures and the disordering can be naturally interpreted as the outcome of the chemical intergrowth between different Friauf polyhedra originating from related Frank−Kasper phases. On the basis of these observations, a new guideline for finding quasicrystals was suggested.

Acknowledgment. The authors would like to thank Prof. S. Lidin for valuable discussions and Prof. H. Yamane and Mr. A. Sato for their assistance during the single crystal measurements. This work was partially funded by the Japan Science and Technology Agency, Solution Oriented Research for Science and Technology (JST-SORST), and by World Premier International Research Center Initiative (WPI Initiative) on Materials Nanoarchitectonics, MEXT, Japan.

Supporting Information Available: CIF file including all crystallographic information for the three title compounds. This material is available free of charge via the Internet at http://pubs.acs.org.

IC800874U